Mater. Res. Soc. Symp. Proc. Vol. 1252 © 2010 Materials Research Society 1252-J02-08

# Fabrication and Current-Voltage Characteristics of Ni Spin Quantum Cross Devices with P3HT:PCBM Organic Materials

Hideo Kaiju[1, 2], Kenji Kondo[1], Nubla Basheer[1], Nobuyoshi Kawaguchi[1], Susanne White[1], Akihiko Hirata[3], Manabu Ishimaru[3], Yoshihiko Hirotsu[3], and Akira Ishibashi[1]
[1] Laboratory of Quantum Electronics, Research Institute for Electronic Science, Hokkaido University, Sapporo 001-0020, Japan
[2] PRESTO, Japan Science and Technology Agency, Saitama 332-0012, Japan
[3] The Institute of Scientific and Industrial Research, Osaka University, Ibaraki, Osaka 567-0047, Japan

## ABSTRACT

We have proposed spin quantum cross (SQC) devices, in which organic materials are sandwiched between two edges of magnetic thin films whose edges are crossed, towards the realization of novel beyond-CMOS switching devices. In SQC devices, nanometer-size junctions can be produced since the junction area is determined by the film thickness. In this study, we have fabricated Ni SQC devices with poly-3-hexylthiophene (P3HT): 6, 6-phenyl C61-butyric acid methyl ester (PCBM) organic materials and investigated the current-voltage (*I-V*) characteristics experimentally and theoretically. As a result of *I-V* measurements, ohmic *I-V* characteristics have been obtained at room temperature for Ni SQC devices with P3HT:PCBM organic materials, where the junction area is as small as 16 nm x 16 nm. This experimental result shows quantitative agreement with the theoretical calculation results performed within the framework of the Anderson model under the strong coupling limit. Our calculation also shows that a high on/off ratio beyond 10000:1 can be obtained in Ni SQC devices with P3HT:PCBM organic materials under the weak coupling condition.

## INTRODUCTION

Molecular electronics have stimulated considerable interest as a technology that may enable a next generation of high-density memory devices [1,2]. Especially, in International Technology Roadmap for Semiconductor (ITRS) 2009 edition, molecular memory devices have been expected as candidates for beyond-CMOS devices since they offer the possibility of nanometer-scale components [3]. Recently, we have proposed spin quantum cross (SQC) devices, in which organic materials are sandwiched between two edges of magnetic thin films whose edges are crossed, towards the realization of novel beyond-CMOS switching devices [4-7]. In SQC devices, the area of the crossed section is determined by the film thickness, in other words 1-20 nm thick films could produce 1×1-20×20 $nm^2$ nanoscale junctions. This method offers a way to overcome the feature size limit of conventional optical lithography and to realize switching devices with a high on/off ratio. Moreover, the resistance of the electrode can be reduced down to ~kΩ since the width of films can be easily controlled to the one as long as ~mm. This makes it possible to detect the resistance of the junction with high sensitivity and to be applied to high-frequency

devices. Thus, SQC devices with organic materials can be expected as novel beyond-CMOS switching devices with high on/off ratios and low-resistance electrodes. In this study, towards the creation of such novel beyond-CMOS devices, we have investigated the resistance properties of Ni electrodes on polyethylene naphthalate (PEN) substrates used in SQC devices and the current-voltage (*I-V*) characteristics of Ni SQC devices with poly-3-hexylthiophene (P3HT): 6, 6-phenyl C61-butyric acid methyl ester (PCBM) organic materials experimentally and theoretically.

## EXPERIMENTS

The fabrication method of SQC devices is shown in figure 1. First, Ni thin films have been thermally evaporated on PEN substrates (2 mm width, 10 mm length, and 20 μm thickness) in a high vacuum chamber at a base pressure of ~$10^{-8}$ torr. The pressure during the evaporation is $10^{-5}$ torr and the temperature near PEN substrates is less than 62 °C, which is lower than the glass transition temperature $T_g$ of 120 °C for PEN substrates. The growth rate is 0.93 nm/min at an evaporation power of 350 W. Then, fabricated Ni/PEN films have been sandwiched between two polymethyl methacrylate (PMMA) resins and the edge of the PMMA/Ni/PEN/PMMA structure has been polished by chemical mechanical polishing (CMP) methods using alumina ($Al_2O_3$) slurries with particle diameters of 0.1, 0.3, and 1.0 μm. Finally, P3HT:PCBM organic materials have been sandwiched between two sets of PMMA/Ni/PEN/PMMA structures whose edges are crossed. The Ni thickness has been measured by an optical method using the diode pumped solid state green laser and the photo diode detector. The microstructures as well as the Ni/PEN interfacial structures have been examined using transmission electron microscopy (TEM) and electron diffraction (ED). The cross-sectional TEM samples have been prepared by a combination of mechanical polishing and Ar ion thinning. The resistance of Ni electrodes has been measured by a two-probe method at room temperature. The *I-V* characteristics of Ni SQC devices with P3HT:PCBM organic materials have been measured by a four-probe method at room temperature.

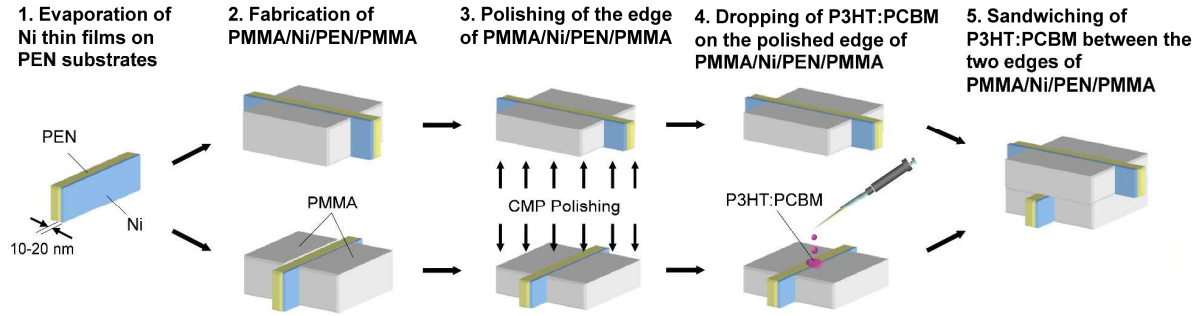


**Figure 1.** Fabrication method of Ni SQC devices with P3HT:PCBM organic materials.

## RESULTS AND DISCUSSION

Figure 2(a) shows the Ni thickness dependence of the electric resistivity for Ni thin films on PEN substrates. The electric resistivity $\rho_{Ni}$ increases with decreasing the Ni thickness. In order to

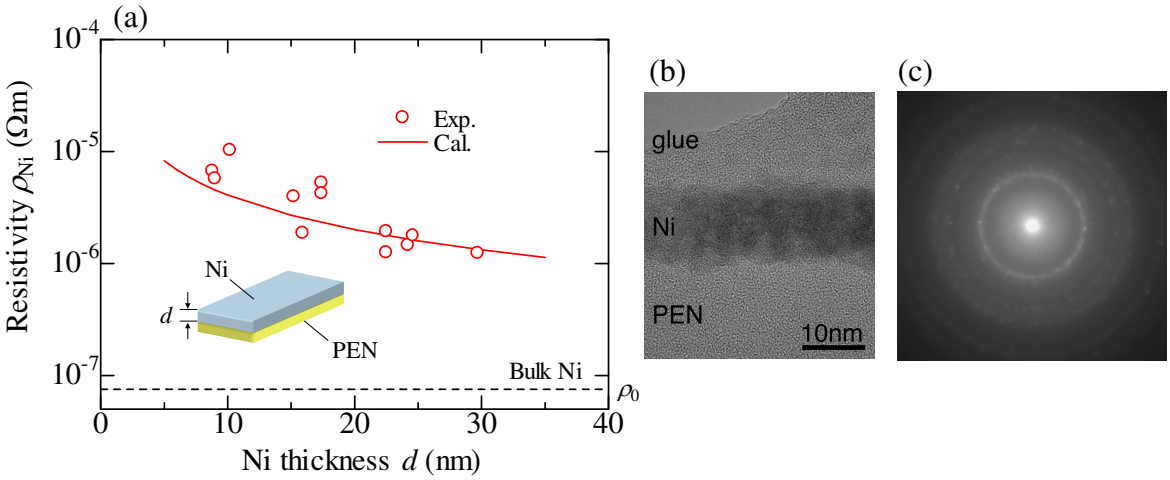


**Figure 2.** (a) Ni thickness dependence of the electric resistivity for Ni/PEN. (b) High-resolution TEM image and (c) ED pattern for Ni (11nm)/PEN.

explain this experimental result quantitatively, we have calculated the electric resistivity using Mayadas-Shatzkes model [8]. According to Mayadas-Shatzkes model, the electric resistivity $\rho_{Ni}$ is expressed by

$$\rho_{Ni} / \rho_0 = \left[1 - \frac{3}{2}\alpha + 3\alpha^2 - 3\alpha^3 \ln(1 + \frac{1}{\alpha})\right]^{-1}, \quad (1)$$

$$\alpha = \frac{\lambda}{D}\frac{R}{1-R}, \quad (2)$$

where $\lambda$ is the electron mean free path, $D$ is the average grain diameter, $R$ is the reflection coefficient for electrons striking the grain boundary, and $\rho_0$ is the electric resistivity for bulk Ni. The electron mean free path $\lambda$ is 11 nm for bulk Ni. The average grain diameter $D$ is 3 nm, which has been obtained from high-resolution TEM image and ED pattern shown in figure 2(b) and (c). The reflection coefficient $R$ is 0.71-0.95, which is the extrapolation value obtained from $R$ in Ni thin films with the thickness of 31-115 nm [9]. From figure 2(a), the experimental result shows good agreement with the calculation result quantitatively. This means that the main contribution to the electric resistivity comes from the electron scattering at grain boundaries in Ni thin films on PEN substrates. Here, we discuss the feasibility of Ni thin films on PEN substrates for the electrodes of SQC devices. As can be seen from figure 2(a), the electric resistivity of Ni thin films on PEN substrates is 1-2 orders larger than that of bulk Ni. However, as we mentioned in the introduction section, the electrode resistance can be reduced since the film width can be controlled to the one as long as ~mm. According to a simple estimation, low-resistance electrodes with 0.1-1 kΩ can be obtained when 10-30 nm thick films are used. Based on this estimation, we have fabricated Ni SQC devices with P3HT:PCBM organic materials and investigated the resistance of Ni electrodes. Figure 3(a) shows the Ni electrode resistance as a function of the line width $l$, which corresponds to the Ni thickness $d$ in SQC devices. The schematic illustration of SQC devices is shown in figure 3(b). In figure 3(a), the Ni electrode resistances in the conventional cross-bar structures are also shown. The black solid line, broken

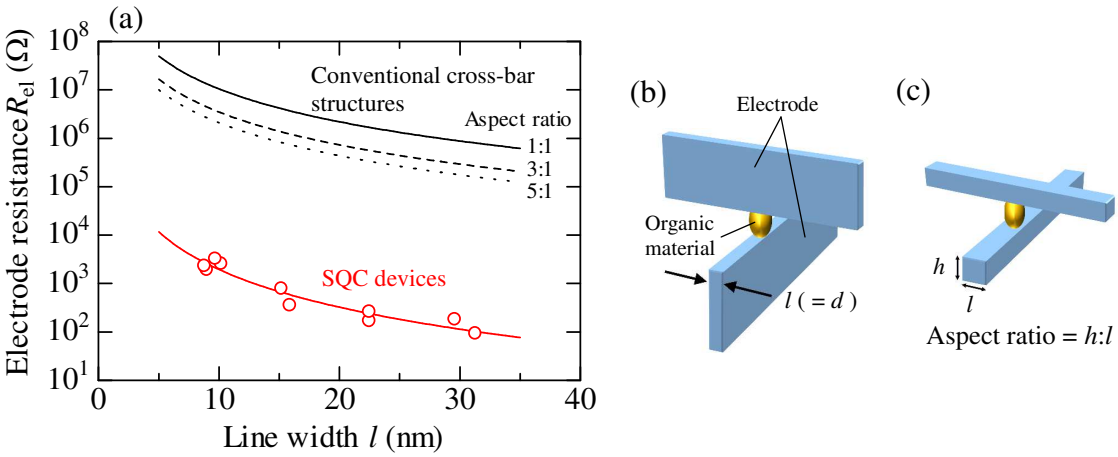


**Figure 3.** (a) Electrode resistance of SQC devices and conventional cross-bar structures. Schematic illustration of (b) SQC devices and (c) conventional cross-bar structures.

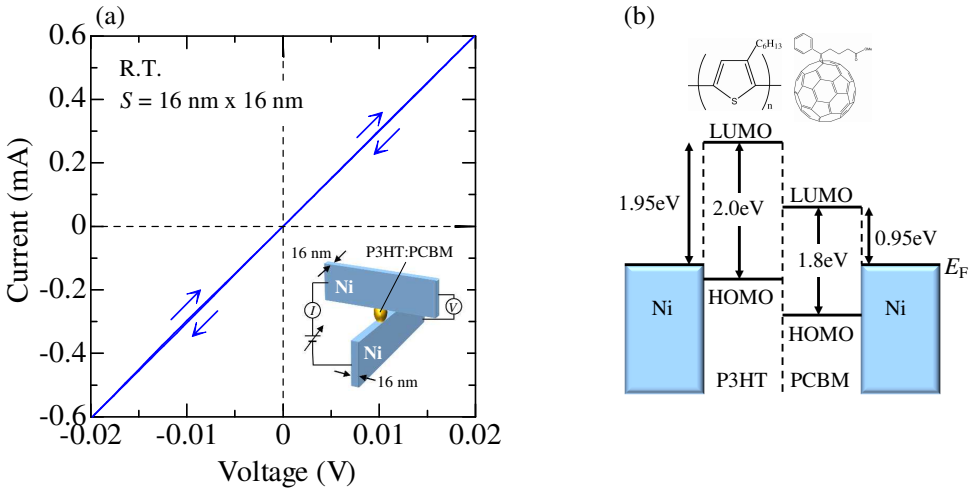


**Figure 4.** (a) *I-V* characteristics and (b) energy diagram for Ni SQCS devices with P3HT: PCBM organic materials.

line, and dotted line represent the Ni electrode resistance estimated in the conventional cross-bar structures with an aspect ratio of 1:1, 3:1, and 5:1, respectively. The schematic illustration of conventional cross-bar structures is shown in figure 3(c). From figure 3(a), the Ni electrode resistance in the conventional cross-bar structures is as large as 1-10 MΩ. In contrast, it is found that the low-resistance electrode with 0.1-1 kΩ can be realized in SQC devices.

Then, we have measured the *I-V* characteristics of SQC devices using these low-resistance electrodes. Figure 4(a) shows the *I-V* characteristics for Ni SQC devices with P3HT:PCBM organic materials at room temperature. The Ni thickness is 16 nm. Therefore, the junction area is as small as 16 nm x 16 nm. We have obtained ohmic characteristics with a junction resistance of 32 Ω. In order to explain this experimental result, we have calculated the *I-V* characteristics of SQC devices within the framework of the Anderson model. The current flowing across the junction in SQC devices can be expressed by

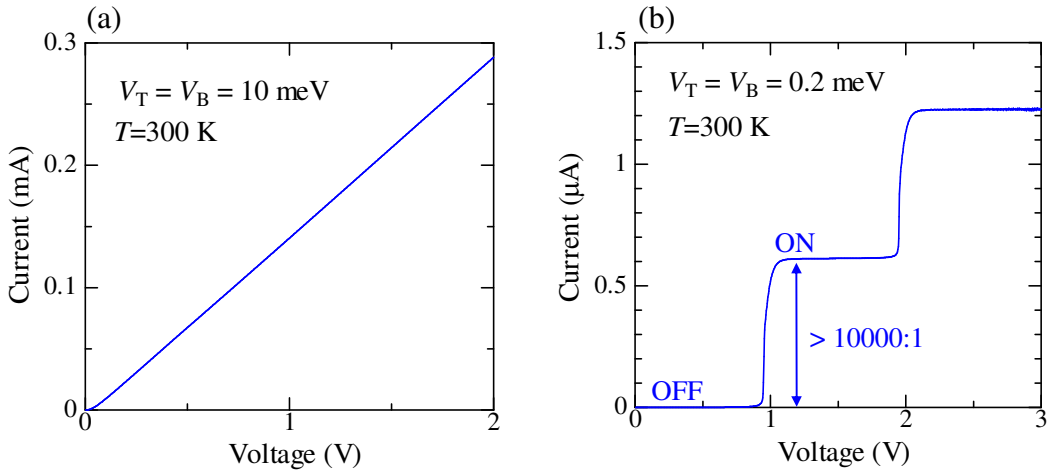


**Figure 5.** Calculated *I-V* characteristics of Ni SQC devices with P3HT:PCBM organic materials (a) under the strong coupling limit and (b) under the weak coupling condition.

$$I = \frac{2e^2}{h}\int_{E_F}^{E_F+eV} d\varepsilon \sum_i \left( \frac{4\Gamma_T(\varepsilon)\Gamma_B(\varepsilon)}{(\varepsilon-\varepsilon_0(i))^2 + (\Gamma_T(\varepsilon)+\Gamma_B(\varepsilon))^2} \right) [f(\varepsilon - eV - E_F) - f(\varepsilon - E_F)] \ , \tag{3}$$

where $e$ is the elementary charge, $h$ is the Planck's constant, $E_F$ is the Fermi energy of Ni, $f(\varepsilon)$ is the Fermi-Dirac distribution function, and $\varepsilon_0(i)$ is the $i$-th energy level of eigen-states for the P3HT:PCBM organic material [7]. We used the value of 9.071 eV for the Ni Fermi level [10], and also assumed that the P3HT:PCBM organic material had two energy levels of $\varepsilon_0(1)$ = 0.95 eV and $\varepsilon_0(2)$ = 1.95 eV, estimated from the Ni Fermi level, as shown in figure 4(b)[11,12]. $\Gamma_{T(B)}$ is the coupling strength between the Ni top (bottom) electrode and the P3HT:PCBM organic material, which is given by

$$\Gamma_{T(B)}(\varepsilon) = \pi D_{T(B)}(\varepsilon) |V_{T(B)}|^2 \ , \tag{4}$$

where $D_{T(B)}$ is a density of states of electrons for the Ni top (bottom) electrode and $V_{T(B)}$ is the coupling constant between the Ni top (bottom) electrode and the P3HT:PCBM organic material. Figure 5(a) shows the calculated *I-V* characteristics of SQC devices under the strong coupling limit. $V_{T(B)}$ is assumed to be 10.0 meV, corresponding to $\Gamma_{T(B)}$ of 3927 meV. We have obtained the ohmic *I-V* characteristics with a resistance of 6.7 kΩ. In this calculation, the junction area is 1 nm x 1 nm, which is expected as a size of one P3HT:PCBM organic molecule, and the number of the conductance channel is four, taking into consideration the spin degeneracy. In experiments, the junction area of P3HT:PCBM organic materials is 16 nm x 16 nm, which corresponds to 1024 (=4x16x16) conductance channels. Therefore, the junction resistance in a size of 16 nm x 16 nm is calculated to be 26 Ω (=6.7kΩ/16/16), which is in good agreement with the experimental value of 32 Ω.

Finally, we have calculated the *I-V* characteristics of SQC devices under the weak coupling condition, shown in figure 5(b). $V_{T(B)}$ is assumed to be 0.2 meV, corresponding to $\Gamma_{T(B)}$ of 1.57 meV. From figure 5(b), the calculated result shows the sharp steps at the positions of the energy level of the P3HT:PCBM organic material. The off-state current $I_0$ is 34.1 pA at the voltage $V_0$

of 0.1 V, and the on-state current $I_1$ is 0.59 $\mu$A at the voltage $V_1$ of 1.05 V. As we estimate the switching on/off ratio, the $I_1/I_0$ ratio is found to be an excess of 10000:1. This indicates that SQC devices under the weak coupling condition can be expected to have potential application in novel switching devices with a high switching ratio.

## CONCLUSIONS

We have fabricated Ni SQC devices with P3HT:PCBM organic materials and investigated the *I-V* characteristics experimentally and theoretically. As a result of *I-V* measurements, ohmic *I-V* characteristics have been obtained at room temperature for Ni SQC devices with P3HT:PCBM organic materials, where the junction area is as small as 16 nm x 16 nm. This experimental result shows quantitative agreement with the theoretical calculation results performed within the framework of the Anderson model under the strong coupling limit. Our calculation also demonstrates that a high on/off ratio beyond 10000:1 can be obtained in Ni SQC devices with P3HT:PCBM organic materials under the weak coupling condition.

## ACKNOWLEDGMENTS

This research has been partially supported by Special Education and Research Expenses from Post-Silicon Materials and Devices Research Alliance, a Grant-in-Aid for Young Scientists from MEXT, Precursory Research for Embryonic Science and Technology program and Research for Promoting Technological Seeds from JST, Foundation Advanced Technology Institute (ATI), and a Grant-in-Aid for Scientific Research from JSPS. The authors would like to express their sincere appreciation to Dr. M. Hirasaka of Teijin Ltd., Research Manager K. Kubo of Teijin DuPont Films Japan Ltd., Prof. M. Yamamoto, Assist. Prof. K. Matsuda, Dr. S. Jin, H. Sato and M. Takei in Hokkaido University for helpful discussions.

## REFERENCES

1. J. Chen, M. A. Reed, A. M. Rawlett, and J. M. Tour, Science **286**, 1550(1999).
2. Y. Chen, D. A. A. Ohlberg, X. Li, D. R. Stewart, R. S. Williams, J. O. Jeppesen, K. A. Nielsen, J. F. Stoddard, D. L. Olynick, and E. Anderson, Appl. Phys. Lett. **82**, 1610 (2003).
3. Semiconductor Industry Association, International Technology Roadmap for Semiconductors (ITRS) 2009 ed.
4. K. Kondo and A. Ishibashi, Jpn. J. Appl. Phys. **45**, 9137 (2006).
5. H. Kaiju, A. Ono, N. Kawaguchi, and A. Ishibashi: J. Appl. Phys. **103**, 07B523 (2008).
6. H. Kaiju, A. Ono, N. Kawaguchi, K. Kondo, A. Ishibashi, J. H. Won, A. Hirata, M. Ishimaru, and Y. Hirotsu: Appl. Sur. Sci. **255**, 3706 (2009).
7. K. Kondo, H. Kaiju, and A. Ishibashi, J. Appl. Phys. **105**, 07D5221 (2009).
8. A. F. Mayadas and M. Shatzkes: Phys. Rev. B **1**, 1382 (1970).
9. C. Nacereddine, A. Layadi, A. Guittoum, S. –M. Cherif, T. Chauveau, D. Billet, J. B. Youssef, A. Bourzami, and M. –H. Bourahli: Mater. Sci. Eng. B **136**, 197 (2007).
10. C. S. Wang and J. Callaway, Phys. Rev. B **15**, 298 (1977).
11. D. E. Eastman, Phys. Rev. B **2**, 1 (1970).
12. B. C. Thompson and J. M. J. Frecht, Angew. Chem. Int. Ed. **47**, 58 (2008).